High Power Laser Science and Engineering, (2024), Vol. 12, e90, 6 pages.
doi:10.1017/hpl.2024.78

HIGH POWER LASER
SCIENCE AND ENGINEERING

LETTER

High-contrast 10 PW laser system at the Extreme Light Infrastructure - Nuclear Physics facility

Olivier Chalus[1], Christophe Derycke[1], Mathilde Charbonneau[1], Stanislas Pasternak[1], Sandrine Ricaud[1], Peter Fischer[2], Valeriu Scutelnic[2], Erhard Gaul[2], Georg Korn[2], Saidbek Norbaev[3], Stefan Popa[3,4], Lidia Vasescu[3], Antonia Toma[3], Gabriel Cojocaru[3], and Ioan Dancus[3]

[1] *Thales LAS France, Elancourt, France*
[2] *Marvel Fusion, Munich, Germany*
[3] *Extreme Light Infrastructure - Nuclear Physics, IFIN-HH, Măgurele, Romania*
[4] *Doctoral School of Physics, University of Bucharest, Bucharest, Romania*

(Received 6 August 2024; revised 21 October 2024; accepted 29 October 2024)

Abstract
We are showing a significant enhancement in the temporal contrast by reducing the coherent noise of the 10 PW laser system at the Extreme Light Infrastructure - Nuclear Physics facility. The temporal contrast was improved by four orders of magnitude at 10 picoseconds and by more than one order of magnitude at 50 picoseconds before the main peak. This improvement of the picosecond contrast is critical for the experiments using thin solid targets.

Keywords: high-power laser; laser diagnostics; temporal contrast

1. Introduction

Temporal contrast is one of the main topics of development for high-peak-power lasers around the world. Lasers that are aiming to deliver high irradiances on target require good control of the temporal contrast to prevent target damage when dealing with ultra-thin solid targets[1] and ensure the desired interaction regime with the main pulse[2].

The Extreme Light Infrastructure - Nuclear Physics (ELI-NP) facility is an open centre for users, dedicated to experiments using high-power lasers for nuclear physics[3,4]. The ELI-NP High Power Laser System (HPLS) is a dual-arm laser system that can deliver 10 PW, 1 PW or 100 TW peak power laser pulses towards five experimental areas[5]. The HPLS at ELI-NP is the first laser in the world to demonstrate the delivery of 10 PW peak power laser pulses to experimental areas[6], opening new frontiers for experimental physics.

Currently, ELI-NP is open for users, with user experimental calls open on the ELI-laser user portal[7].

Correspondence to: I. Dancus, Extreme Light Infrastructure - Nuclear Physics, IFIN-HH, Reactorului 30, Magurele 077125, Romania. Email: ioan.dancus@eli-np.ro

A thorough study of the pedestal of the main pulse in chirped pulse amplifier (CPA) lasers has been led at the Laboratory of Laser Energetics and the University of Rochester by Bromage *et al.*[8] and Dorrer and Bromage[9]. They have demonstrated that a convex mirror placed in the focus within the Offner-type stretcher contributes to the contrast degradation, part of the pedestal, scaling proportionally to the surface roughness quality of that mirror[10]. This type of contrast degradation is described now as the spectral random phase noise or coherent noise.

Ranc *et al.*[11] demonstrated on the Apollon laser a contrast improvement with an ultralow roughness mirror. It was shown that a mirror with a roughness of 0.17 nm root mean square (RMS) leads to a significant reduction of the pedestal around the main pulse.

An extensive study of different sources of contrast degradation was performed by Kiriyama *et al.*[12] for the J-KAREN-P Petawatt Laser. They show an improvement of the temporal contrast by addressing each of these degradation sources carefully.

One of the main contributors to random phase noise contrast degradation is the placement of optical elements in the focus of the Offner-type stretcher. Lu *et al.*[13] reported on the possibility of replacing the Offner-type stretcher

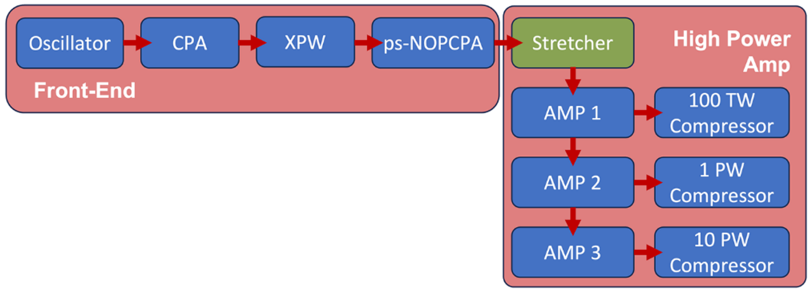

Figure 1. Schematic diagram of the ELI-NP HPLS. Marked with green is the stretcher that was updated during the activities reported here.

with a design based on two concave mirrors that avoid this drawback. The design of a stretcher with cylindrical optics has also been proposed[14].

One alternative strategy to enhance the on-target contrast of a high-power laser is the integration of a plasma mirror. Choi *et al.*[15] demonstrated a high reflectivity of 70% for a plasma mirror integrated into the 4 PW laser system at CoReLS, resulting in a high-contrast enhancement factor of 700,000.

In this work, we present a comparative study of the temporal contrast for three configurations of the stretcher implemented in the same 10 PW CPA laser system at ELI-NP. The first configuration utilizes an Offner-type stretcher with a regular convex mirror. The second configuration employs the same Offner-type stretcher, integrating a highly polished mirror. The third configuration incorporates a reflecting Martinez-type stretcher. This comparative study holds significant relevance for developing appropriate temporal contrast enhancement techniques for existing high-power laser systems and for the design of future high-power laser systems currently under development.

2. The Extreme Light Infrastructure - Nuclear Physics High Power Laser System

The ELI-NP HPLS is a dual-arm hybrid CPA–optical parametric chirped pulse amplifier (OPCPA) laser system extensively described in Ref. [5]. The laser system starts with a front-end seeded by a broadband Venteon (Laser Quantum) oscillator followed by a CPA based on regenerative geometry. The next subsystems of the front-end are used to clean the temporal contrast and prepare the pulses for high-energy amplification. They are composed of a cross-polarized wave generation filter and a dual-stage picosecond non-collinear optical parametric chirp pulse amplifier (ps-NOPCPA). At the output of the front-end, the energy per pulse is of the order of 10 mJ with a temporal contrast of more than 12 orders of magnitude at more than 15 ps from the main pulse. The pulses after the front-end are split to seed each of the arms of the HPLS high-energy amplifiers. Each of these arms is composed of a stretcher, a spectral phase control system based on an acousto-optic programmable dispersion filter (Dazzler from Fastlite), multiple amplification stages and output pulse compressors. A schematic diagram of the ELI-NP HPLS is presented in Figure 1.

For the improvement of the contrast of the HPLS, we decided to use two approaches: firstly, the improvement of the roughness of the convex mirror in the existing Offner-type stretcher and, secondly, by using a Martinez-type design. This work was done on the stretcher used in the high-power amp part of the ELI-NP HPLS (marked with the green colour in Figure 1).

3. Ultrahigh-quality convex mirror in the Offner-type stretcher

The initial design of the ELI-NP HPLS stretcher is a two-grating Offner type described also in Refs. [5,16]. Figure 2 shows a schematic diagram of this stretcher, which uses two gratings with a line density of 1480 lines/mm at a 56° angle of incidence. The roof mirrors ensure four passes of the beam through this configuration. As for the Offner

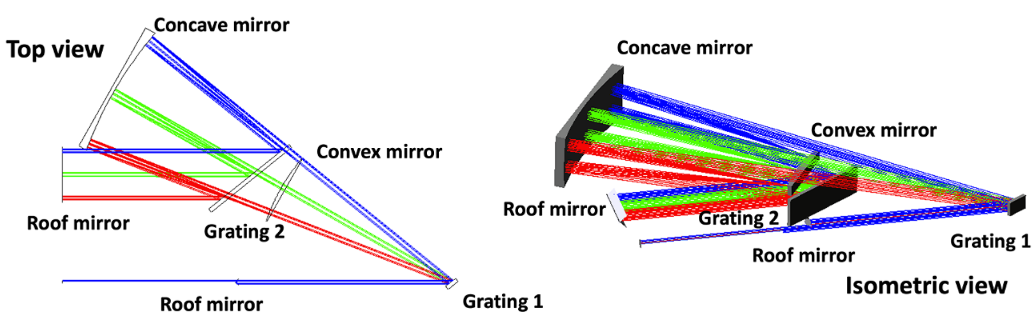

Figure 2. Schematic diagram of the Offner-type stretcher implemented at the ELI-NP HPLS.

https://doi.org/10.1017/hpl.2024.78 Published online by Cambridge University Press

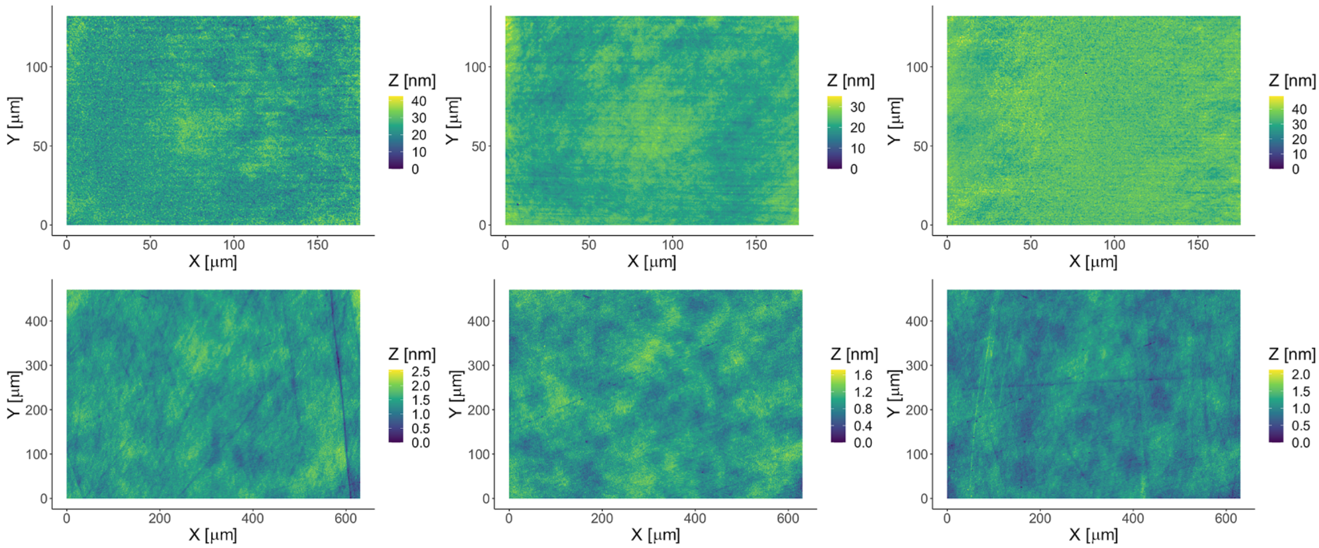

Figure 3. Roughness measurements for the old mirror (top row) and new, highly polished mirror (bottom row) performed on three separate locations.

configuration, the stretcher uses one concave mirror and one convex mirror. The radius of curvature for these mirrors is 1200 and –600 mm respectively. The Offner stretcher under this configuration presents the advantages of being compact as well as generating minimum spectral aberrations and chirp. To correct the spectral random phase noise temporal contrast degradation at ELI-NP, we decided to replace the convex mirror of the PW temporal stretcher with an ultra-low roughness one.

The new ultra-low roughness mirror was produced by Thales SESO France using the QED magnetorheological fluid polishing method for its final polishing[17]. The RMS roughness of the new ultra-low roughness mirror is 0.2 nm in comparison with the RMS roughness of the old 'regular' mirror of 3.5 nm. Figure 3 presents three representative on-axis measurements of the roughness for each of the two convex mirrors.

4. New stretcher design

The HPLS compressor is fixed, enabling it to compensate for a fixed dispersion [5]. The existing Offner-type stretcher is optimized to match the compressor dispersion. Consequently, the design of the new stretcher must match, as closely as possible, the output parameters of the existing Offner-type stretcher to closely match the dispersion of the compressor. To achieve a Fourier transform limited pulse at the output of the laser system, the dispersion parameters can be precisely adjusted using the Dazzler equipment.

The proposed stretcher offers both advantages: a transmission efficiency two times higher than the Offner configuration due to its design, and the utmost advantage of eliminating any optics in the far-field of the spectral domain. This enables the removal of the spatial–spectral coupling at the origin of the pedestal of the main pulse.

The spectral band of the new stretcher is over 130 nm centred at 810 nm. The stretching factor is 14.5 ps/nm. The clear aperture is 5 mm and the incident angle on the gratings is set to 56°. The gratings groove density is 1480 lines/mm.

The new stretcher design is a reflective Martinez-type stretcher with two similar converging mirrors. A similar design was first proposed by Rudd *et al.*[18] and also used by Lu *et al.*[13]. A schematic, ray tracing and diagram of the new stretcher are shown in Figure 4. The converging mirrors are spherical mirrors with a radius of curvature of 2000 mm. As one can see in the side view of Figure 4, the spherical mirrors

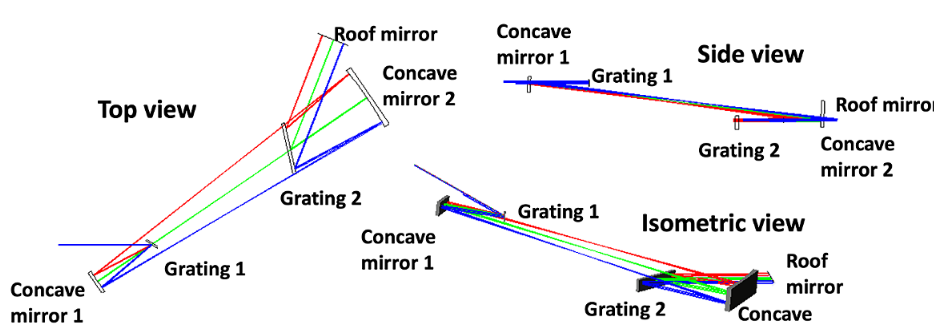

Figure 4. Schematic diagram of the new reflective Martinez-type stretcher implemented at the ELI-NP HPLS.

https://doi.org/10.1017/hpl.2024.78 Published online by Cambridge University Press

are tilted from the terrestrial vertical plane, M1, by 2° and M2 by 2.8°. The design of the stretcher has been optimized to limit all the spectral aberrations and spatial chirp to get as close as possible to the performance of the original Offner stretcher[19,20].

5. Results and discussion

Figure 5 shows the results obtained for the temporal contrast measurement using a Tundra cross-correlator for the three cases: an Offner-type stretcher using a regular convex mirror; the same Offner-type stretcher using the ultra-low roughness convex mirror; and the reflective Martinez-type stretcher. All these measurements were performed using the same laser system and the same measurement tools to showcase the impact of the different types of stretchers on the temporal contrast.

The measurements from Figure 5 were performed at 1 Hz repetition rate, with AMP 1 and AMP 2 running in nominal specifications, using a cross-correlator (Tundra from UltraFast Innovation). After AMP 2, the beam propagated in the nominal configuration, through AMP 3, the compressor and the diagnostic bench. For these measurements, amplifier AMP 3 was not pumped as its repetition rate of 1 pulse per minute as that would prevent one from performing a scanning measurement on a reasonable timescale.

In both the ultrahigh-quality convex and reflective Martinez-type implementations, a strong, well-defined peak can be observed at approximately 9 ps. This peak is not visible on the regular quality convex mirror Offner-type stretcher curve because the pedestal masks it. We identify this peak origin in a prism/transmission grating bulk dispersion compensation device that is integrated into the system. These pre-pulses are generated by the transmission grating that is part of this bulk dispersion compensation device. The device introduces a post-pulse as a consequence of multiple reflections on the faces of the transmission grating. During the amplification of the pulses, by nonlinear coupling in the amplifying crystals, the post-pulse is transformed into a pre-pulse. We are working on resolving this issue by replacing the face parallel transmission grating with a slightly wedged one.

Looking at the general feature of the pedestal, one can observe a clear improvement from the regular convex Offner stretcher to the ultrahigh-quality convex Offner stretcher. At 10 ps this improvement is of three orders of magnitude. The improvement starts from the main pulse and it is visible up to the 50 ps range, where it is about half an order of magnitude.

The improvement introduced by the reflective Martinez-type stretcher compared to the Offner-type ultrahigh-quality convex stretcher is less dramatic but significant. This improvement is about one order of magnitude at the 10 ps position and is, in general, of one to half an order of magnitude up to the 50 ps range. This is an unprecedentedly high level of contrast for multi-PW systems 10 orders of magnitude at 10 ps before the main pulse.

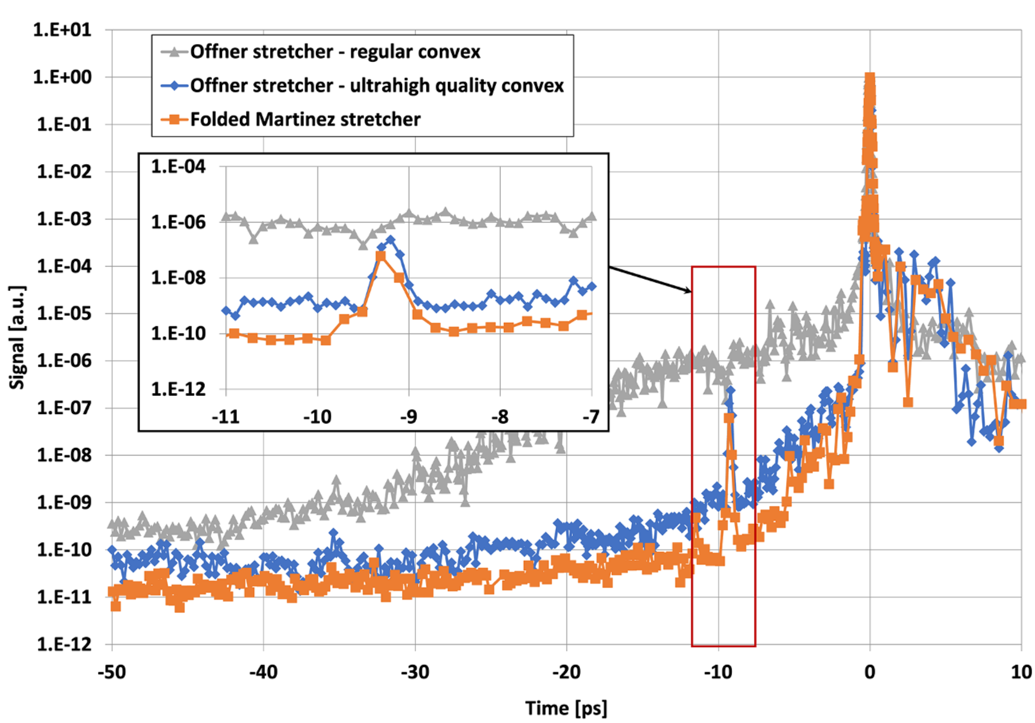

Figure 5. Contrast measurement curves for the three cases: grey curve, Offner-type stretcher using a regular convex mirror; blue curve, Offner-type stretcher using an ultrahigh-quality convex mirror; orange curve, reflective Martinez-type stretcher. The peak at approximately 9 ps is generated by a bulk dispersion compensator. The inset provides a clearer representation of the position of the approximately 9 ps pre-pulses, thereby revealing the sampling rate of the measuring device and the peaks with similar relative positions.

https://doi.org/10.1017/hpl.2024.78 Published online by Cambridge University Press

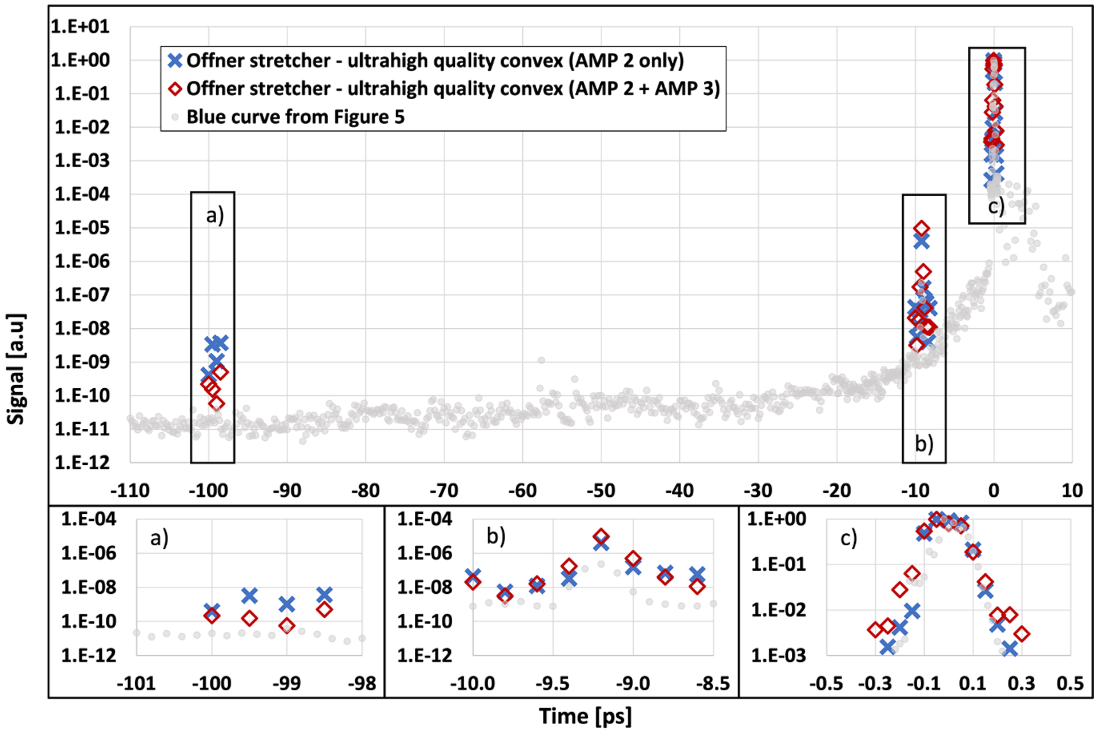

Figure 6. Contrast measurement at 1 shot per minute, showing similar contrast obtained with AMP 3 running at nominal parameters to the measurements presented in Figure 5: blue cross, similar conditions to that in the Figure 5 blue curve (no pump on AMP 3); red rhomb, similar to the previous and with AMP 3 pumped; grey circle, reproduction of the blue curve from Figure 5 for comparison. The difficulty of optimizing the alignment at a low repetition rate leads to a lower dynamic range obtained for these measurements in comparison to the one presented in Figure 5. The inset plots show details of the measurement of the –100 ps region (a), of the pre-pulse at approximately 9 ps (b) and of the main pulse (c).

The nominal dynamic range of the measurement device used is 11 orders of magnitude. It can be observed from Figure 5 that this may be the limiting factor for the obtained value of the contrast using the reflective Martinez stretcher for ranges higher than –30 ps.

To verify that pumping of AMP 3 will not lead to a degradation of the contrast compared with the measurements presented in Figure 5, we measured the contrast at few points using the nominal pumping level at 1 shot per minute repetition rate. The results are presented in Figure 6. One can observe that due to the alignment optimization difficulties at this repetition rate, we were unable to reach the same value of dynamic range for these measurements. When AMP 3 is activated, an attenuation is implemented between the amplifier and the compressor to achieve a level of energy output at the compressor similar to the 1 Hz setup. This attenuation introduces a slight misalignment in the far-field, resulting in a reduction of the dynamic range that can be obtained with the Tundra cross-correlator. This misalignment is challenging to correct at a repetition rate of 1 shot per minute, leading to the degradation of dynamic range in the full energy measurements. Nevertheless, it can be seen that there is no degradation of the contrast when AMP 3 is running at the nominal parameters.

The temporal contrast measurement performed by the Tundra device is a far-field contrast measurement. Assuming the temporal features are preserved in the far-field of the focusing optics in the experimental chamber, it is expected that a peak irradiance of 10^{23} W/cm^2 with a level of 10^{13} W/cm^2 at 10 ps before the main pulse can be obtained on target. This will allow an unperturbed interaction of the laser and ultra-thin targets.

6. Conclusions

In conclusion, we demonstrated the importance of the coherent spectral noise on the degradation of the contrast in CPA laser systems by using three stretcher configurations: two Offner-type stretchers with two different roughness convex mirrors and one reflective Martinez-type stretcher. The contrast of the ELI-NP HPLS was improved by four orders of magnitude at 10 ps when using the reflective Martinez-type stretcher compared with the standard roughness convex mirror Offner-type stretcher used during the commissioning of the laser system. This improvement is set to open the HPLS to experiments on ultra-thin solid targets by preventing degradation that is usually caused by the leading edge of the high-power pulse.

Acknowledgements

This work was supported by the PN 23 21 01 05 and the LASCOMB ELI-Ro contracts funded by the Romanian Ministry

https://doi.org/10.1017/hpl.2024.78 Published online by Cambridge University Press

of Research, Innovation and Digitalization and the IOSIN 2023 funds for research infrastructures of national interest.

The authors thank the Apollon Team at LULI and in particular Dimitris Papadopoulos and Bruno LeGarrec for the fruitful discussion and help with the design of the new stretcher. The authors also thank Samy Ferhat for the preliminary experimental tests performed on the new stretcher.

References

1. G. Cantono, A. Permogorov, J. Ferri, E. Smetanina, A. Dmitriev, A. Persson, T. Fulop, and C.-G. Wahlstrom, Sci. Rep. **11**, 5006 (2021).
2. J. Psikal, Plasma Phys. Controll. Fusion **66**, 045007 (2024).
3. S. Gales, K. A. Tanaka, D. L. Balabanski, F. Negoita, D. Stutman, O. Tesileanu, C. A. Ur, D. Ursescu, I. Andrei, S. Ataman, M. O. Cernaianu, L. D'Alessi, I. Dancus, B. Diaconescu, N. Djourelov, D. Filipescu, P. Ghenuche, D. G. Ghita, C. Matei, K. Seto, M. Zeng, and N. V. Zamfir, Rep. Progress Phys. **81**, 094301 (2018).
4. K. A. Tanaka, K. M. Spohr, D. L. Balabanski, S. Balascuta, L. Capponi, M. O. Cernaianu, M. Cuciuc, A. Cucoanes, I. Dancus, A. Dhal, B. Diaconescu, D. Doria, P. Ghenuche, D. G. Chita, S. Kisyov, V. Nastasa, J. F. Ong, F. Rotaru, D. Sangwan, P.-A. Soderstrom, D. Stutman, G. Suliman, O. Tesileanu, L. Tudor, N. Tsoneva, C. A. Ur, D. Ursescu, and N. V. Zamfir, Matter Radiat. Extremes **5**, 024402 (2020).
5. F. Lureau, G. Matras, O. Chalus, C. Derycke, T. Morbieu, C. Radier, O. Casagrande, S. Laux, S. Ricaud, G. Rey, A. Pellegrina, C. Richard, L. Boudjemaa, C. Simon-Boisson, A. Baleanu, R. Banici, A. Gradinariu, C. Caldararu, B. De Boisdeffre, P. Ghenuche, A. Naziru, G. Kolliopoulos, L. Neagu, R. Dabu, I. Dancus, and D. Ursescu, High Power Laser Sci. Eng. **8**, e43 (2020).
6. C. Radier, O. Chalus, M. Charbonneau, S. Thambirajah, G. Deschamps, S. David, J. Barbe, E. Etter, G. Matras, S. Ricaud, V. Leroux, C. Richards, F. Lureau, A. Baleanu, R. Banici, A. Gradinariu, C. Caldararu, C. Capiteanu, A. Naziru, B. Diaconescu, V. Iancu, R. Dabu, D. Ursescu, I. Dancus, C. A. Ur, K. A. Tanaka, and N. V. Zamfir, High Power Laser Sci. Eng. **10**, e21 (2022).
7. https://up.elilaser.eu/calls.
8. J. Bromage, C. Dorrer, and R. K. Jungquist, J. Opt. Soc. Am. B **29**, 1125 (2012).
9. C. Dorrer and J. Bromage, Opt. Express **16**, 3058 (2008).
10. G. Cheriaux, P. Rousseau, F. Salin, J. P. Chambaret, Barry Walker, and L. F. Dimauro, Opt. Lett. **21**, 414 (1996).
11. L. Ranc, C. Le Blanc, N. Lebas, L. Martin, J.-P. Zou, F. Mathieu, C. Radier, S. Ricaud, F. Druon, and D. Papadopoulos, Opt. Lett. **45**, 4599 (2020).
12. H. Kiriyama, Y. Miyasaka, A. Kon, M. Nishiuchi, A. Sagisaka, H. Sasao, A. S. Pirozhkov, Y. Fukuda, K. Ogura, K. Kondo, N. Nakanii, Y. Mashiba, N. P. Dover, L. Chang, M. Kando, S. Bock, T. Ziegler, T. Püschel, H.-P. Schlenvoigt, K. Zeil, and U. Schramm, Photonics **10**, 997 (2023).
13. X. Lu, H. Zhang, J. Li, and Y. Leng, Opt. Lett. **46**, 5320 (2021).
14. J. Bromage, M. Millecchia, J. Bunkenburg, R. K. Jungquist, C. Dorrer, and J. D. Zuegel, in 2012 *Conference on Lasers and Electro-Optics (CLEO)* (2012), paper CM4D.4.
15. I. W. Choi, C. Jeon, S. G. Lee, S. Y. Kim, T. Y. Kim, I. J. Kim, H. W. Lee, J. W. Yoon, J. H. Sung, S. K. Lee, and C. H. Nam, Opt. Lett. **45**, 6342 (2020).
16. J. Jiang, Z. Zhang, and T. Hasama, J. Opt. Soc. Am. B **19**, 678 (2002).
17. D. C. Harris, Proc. SPIE **8016**, 80160N (2011).
18. J. V. Rudd, G. Korn, S. Kane, J. Squier, G. Mourou, and P. Bado, Opt. Lett. **18**, 2044 (1993).
19. O. Chalus, D. Papadopoulos, F. Mathieu, P. Audebert, N. Lebas, M. Charbonneau, S. Pasternak, C. Derycke, S. Ferhat, A. Pellegrina, S. Ricaud, B. LeGarrec, E. Gaul, G. Cojocaru, A. Toma, S. Norbaev, and I. Dancus, in *10th International Conference on Ultrahigh Intensity Lasers* (2024), p. 129.
20. O. Chalus, D. Papadopoulos, F. Mathieu, P. Audebert, N. Lebas, M. Charbonneau, S. Pasternak, C. Derycke, S. Ferhat, A. Pellegrina, S. Ricaud, and B. LeGarrec, "Picosecond contrast improvement for PW class lasers based on modified stretcher design," in preparation (2024).